

# Effect of parameters setting on performance of discrete component removal (DCR) methods for bearing faults detection

Bovic Kilundu<sup>1</sup>, Agusmian Partogi Ompusunggu<sup>2</sup>, Faris Elasha<sup>3</sup>, and David Mba<sup>4</sup>

<sup>1,2</sup> *Flanders Mechatronics Technology Centre, Leuven, 3001, Belgium*

*bovic.kilunduyebondo@fmtc.be*

*agusmian.ompusunggu@fmtc.be*

<sup>3,4</sup> *School of Engineering- Cranfield University, Cranfield, Beds MK43 0AL, UK*

*f.elasha@cranfield.ac.uk*

*D.Mba@cranfield.ac.uk*

## ABSTRACT

Separation between non-deterministic and deterministic components of gearbox vibration signals has been considered as important signal processing step for rolling-element bearing fault diagnostics. In this paper, the performance of bearing fault detection after applying various discrete components removal (DCR) methods is quantitatively compared. Three methods that have become widely used, namely (i) time synchronous average, (ii) self adaptive noise cancellation (SANC) and (iii) cepstrum editing, were considered. The three DCR methods with different parameter settings have been applied to vibration signals measured on two different gearboxes. In general, the experimental results show that cepstrum editing method outperforms the other two methods.

## 1. INTRODUCTION

Detecting bearing faults on rotating machinery based on vibration signals is often a challenge due to the high energy (dominating) signals; originating from various machine elements including gears, screws, and shafts; that can mask weak signals (i.e. non-deterministic) generated by bearing faults. These dominant signals are deterministic, meaning that they will appear as discrete components in the frequency domain. When bearing faults detection is of interest, it is therefore important to remove these discrete components prior to applying further signal processing. Several methods have been proposed in literature for separating discrete components and non-deterministic components (i.e. residual signals) useful for bearing fault detection. Recently R. Randall and Sawalhi (2011) have presented a new method for separating discrete components from a signal based on cepstrum editing. The

choice of setting parameters when applying these methods can have a significant effect on the residual signals. A qualitative comparison of different methods has also been recently performed by R. Randall et al. (2011). However, to the authors' knowledge, the effects of different parameters setting on the performance of bearing fault detection have not been discussed yet elsewhere. To fill this gap, this paper aims at discussing the effects of parameters setting and eventually providing a quantitative comparison. The performance of bearing fault detection after applying different DCR methods is analyzed. Here, two other methods are evaluated and compared to the cepstrum editing method, namely synchronous average and synchronous adaptive noise cancellation (SANC).

The paper first presents the 3 discrete component removal (DCR) methods and discusses adjustable parameters for each one, and second, applies the methods to vibration signals measured on two gearboxes: (i) an industrial gearbox which is a part of a transmission driveline on the actuation mechanism of secondary control surface in civil aircraft and (ii) a laboratory gearbox used in the PHM09 data competition. The residual signals obtained from these three methods are processed following the optimized envelope analysis by using spectral kurtosis for determining the optimal frequency band for demodulation. Bearing detection performance is assessed on the envelope spectrum.

## 2. DISCRETE COMPONENT REMOVAL METHODS (DCR)

There exist a number of methods for separating signal components with different pros and cons, such as time synchronous averaging (TSA), linear prediction, adaptive and self-adaptive noise cancellation (SANC), discrete/random separation (DRS), and the recently developed method, i.e. cepstral editing. The three methods considered in this work are briefly discussed in the following subsections.

B. Kilundu et al. This is an open-access article distributed under the terms of the Creative Commons Attribution 3.0 United States License, which permits unrestricted use, distribution, and reproduction in any medium, provided the original author and source are credited.

### 2.1. Synchronous adaptive noise cancellation (SANC)

SANC is an adaptive filtering method where the filter coefficients  $\mathbf{w}$  are adaptively updated according to the scheme shown in Figure 1. The filter coefficients are updated such that the prediction error  $e(n)$  obtained by subtracting the filtered signal  $y(n)$  from the original signal  $x(n)$  is minimized. The input of the filter  $\mathbf{d}(n)$  is a delayed version of the original signal. SANC allows separation between deterministic and non-deterministic signals. The reason is that a non-deterministic signal is not correlated to previous sample unlike deterministic signal. However, one needs to ensure that the delay should be greater than the time of decorrelation of the non-deterministic signal but it should exceed the decorrelation time of the deterministic part. The filter output  $y(n)$  is the *deterministic signal* containing gears and shaft signals and the output error represents the *non-deterministic part* containing bearing signals

The most used adaptation algorithm is the celebrated least mean-square (LMS) developed by Widrow and Hoff (Widrow, Hoff, et al., 1960). It is characterized by its robustness and a low computational complexity. Its recursive procedure computes the output of the filter and compares it to the original signal. The error is used to adjust the filter coefficient as shown in Eq. (1)

$$\mathbf{w}(n+1) = \mathbf{w}(n) - \mu \cdot e(n) \cdot \mathbf{d}(n) \quad (1)$$

where

$y(n) = \mathbf{w}^T \mathbf{d}$  is the filter output,

$e(n) = x(n) - y(n)$  is the output error,

$d(n)$  is the delayed signal,

$\mathbf{w}(n) = [w_0(n), w_1(n), \dots, w_{M-1}]^T$  are the filter coefficients at the time index  $n$ ,

$\mathbf{x}(n) = [x(n), x(n-1), \dots, x(n-M+1)]^T$  is the input signal,

$\mu$  is the step size parameter that must be selected properly to control stability and convergence.

The use of SANC implies the choice of 3 parameters and its performance relies on them:

- the prediction depth or time delay  $L$
- the step size  $\mu$
- the filter length  $M$

Antoni and Randall (2004) have discussed optimal settings of these parameters giving general guidelines, also presented in (R. Randall et al., 2011). The delay  $L$  should be chosen large enough to exceed the memory of the noise but not so long to destroy the correlation, which can be a bit disturbed in case of slight speed fluctuation. The length of the filter  $M$  should not exceed the signal length to have enough time for adaptation. The step size  $\mu$  represents the convergence rate and will be a trade off between the desired accuracy and the computational cost. A low step size value results in high accuracy.

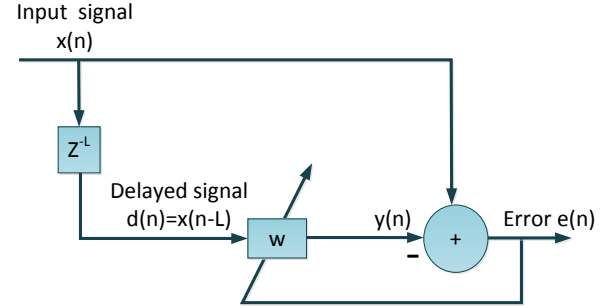


Figure 1. SANC filter process.

### 2.2. Time synchronous average (TSA)

Time Synchronous average (TSA) is a signal processing method aiming at extracting components from a signal that are phase-locked to the shaft revolution by means of averaging several signal segments. The segments can represent one or several shaft revolutions. TSA cancels or significantly reduces the presence of non-synchronous phenomena, which can comprise bearing signals and background (white) noise. In order to perform TSA, the shaft position information is needed for re-sampling the signal in the angular domain. This information can be retrieved from a tachometer or encoder signal. If the tachometer is not located on the shaft of interest, transformation is needed to convert angular positions of the shaft with the tachometer to angular position of the shaft of interest.

In the absence of tachometer signal, Bonnardot et al. (2005) have reported a technique allowing TSA using a virtual tachometer signal generated from accelerometer signal. However, this tachometer-less technique presents some limitations since it requires a very low variation of the speed. TSA can also be used for discrete component removal by subtracting the synchronous signal from the original signal. The remaining or the residual signal contains non-deterministic components comprising bearing signals. The adjustable parameter is the number of average which is related to the number of revolutions in averaged segments.

### 2.3. Cepstrum editing

The cepstrum editing method gives some advantages compared with all the techniques noted previously. One notable advantage of the editing cepstral method is that it can be used to remove the selected frequency components in one operation, without order tracking as long as the speed variation is limited, but it can leave some periodic components if desired. In some applications where the sidebands are not harmonics of the shaft speed, families of uniformly spaced sidebands can be removed with the editing cepstral method. The detailed explanation and the performance of the latter method can be found in (R. Randall & Sawalhi, 2011). The following paragraphs will briefly revisit the method.

Let  $y$  be the measured vibration signal and  $Y(f)$  be the corresponding frequency domain signal. By definition, the cepstrum of this signal  $C(\tau)$  is calculated by taking the inverse Fourier transform of the logarithm of  $Y(f)$ , i.e.

$$C(\tau) = \mathcal{F}^{-1} [\log(Y(f))], \quad (2)$$

with  $\mathcal{F}^{-1}$  denoting the inverse Fourier operation.

In the same way that the word "cepstrum" was coined from "spectrum" by reversing the first syllable, the term "quefrequency" is used for the x-axis of the cepstrum (even though it is time), "rahmonic" means a series of equally spaced peaks in the cepstrum domain (resulting from a series of harmonics or sidebands in the log spectrum) and "lifter" represents a filter applied to the cepstrum (Bogert, Healy, & Tukey, 1963).

Based on the cepstrum definition, it is quite simple to deduce the rationale behind the editing cepstral based DCR method. Given the fact that in the frequency domain, the response signal  $Y(f)$  is a multiplication of the excitation signal  $X(f)$  and the frequency response function  $H(f)$ , i.e.

$$Y(f) = X(f) \times H(f), \quad (3)$$

by taking the logarithm of the response signal  $Y(f)$ , Eq. (3) can thus be written as:

$$\log(Y(f)) = \log(X(f)) + \log(H(f)). \quad (4)$$

Furthermore, by taking the inverse Fourier transform of Eq. (4):

$$\mathcal{F}^{-1} [\log(Y(f))] = \mathcal{F}^{-1} [\log(X(f))] + \mathcal{F}^{-1} [\log(H(f))]. \quad (5)$$

It is clear now from Eq. (5) that in the cepstrum domain, the excitation signal and the transfer path are additive. This implies that the unwanted excitation signal (e.g. gear and shaft related signals) can be removed (i.e. edited) in the cepstrum domain. The cepstral editing based DCR method developed by (R. Randall & Sawalhi, 2011; Sawalhi & Randall, 2011) is schematically shown in Figure 2.

Figure 3 further illustrates the editing process in the cepstrum domain. To remove unwanted rahmonics corresponding to periodic components (i.e. gear signals), the lifter width  $\Delta$  should be chosen appropriately. Up to now, there is no an automatic way for determining the lifter width  $\Delta$ . The (constant) width is typically selected visually based on inspection of the resulting signal.

### 3. EXPERIMENTAL STUDY

#### 3.1. Description of test rigs

To compare the cepstrum editing DCR method to TSA and SANC and assess the effect of parameters setting on performance for bearing faults detection, two sets of experimental

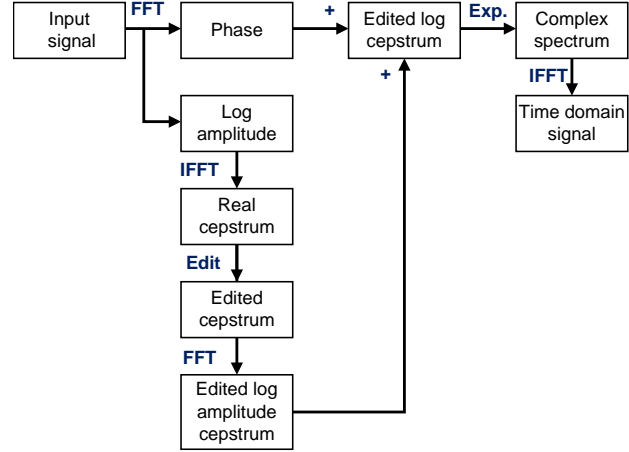


Figure 2. Schematic diagram of the editing cepstral method for removing selected families of harmonics and/or sidebands from time domain signals, reproduced from (R. Randall & Sawalhi, 2011).

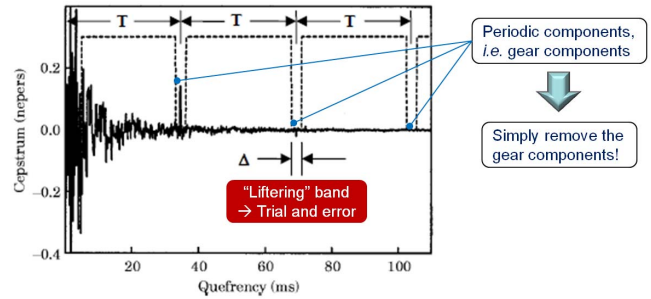


Figure 3. Liftering to remove unwanted rahmonics, reproduced from (Gao & Randall, 1996).

data from gearboxes are used (hereafter called dataset#1 and dataset#2).

#### 3.1.1. Test rig#1

Dataset#1 is measured on an industrial gearbox which is a part of a transmission driveline of the actuation mechanism of secondary control surface in civil aircraft shown in Figure 4. The test rig was designed to simulate the actual operation conditions during the life cycle of the aircraft control system which implies the gearbox would experience a range of speed and torque conditions. It is driven by an electrical motor. A second motor acted as a generator is used to apply load to the system. The nominal speed of the motor is 710 rpm. The gearbox consists of two spur bevel gears, each with 17 teeth producing a gear ratio of 1:1. Two angular contact bearings are used to support the gears.

The characteristic bearing fault frequencies for the operating speed of 60 rpm (1 Hz) and for the operating speed of 710 rpm (11.83 Hz) including, (i) ball pass frequency of inner race (BPFI), (ii) ball pass frequency of outer race (BPFO), ball

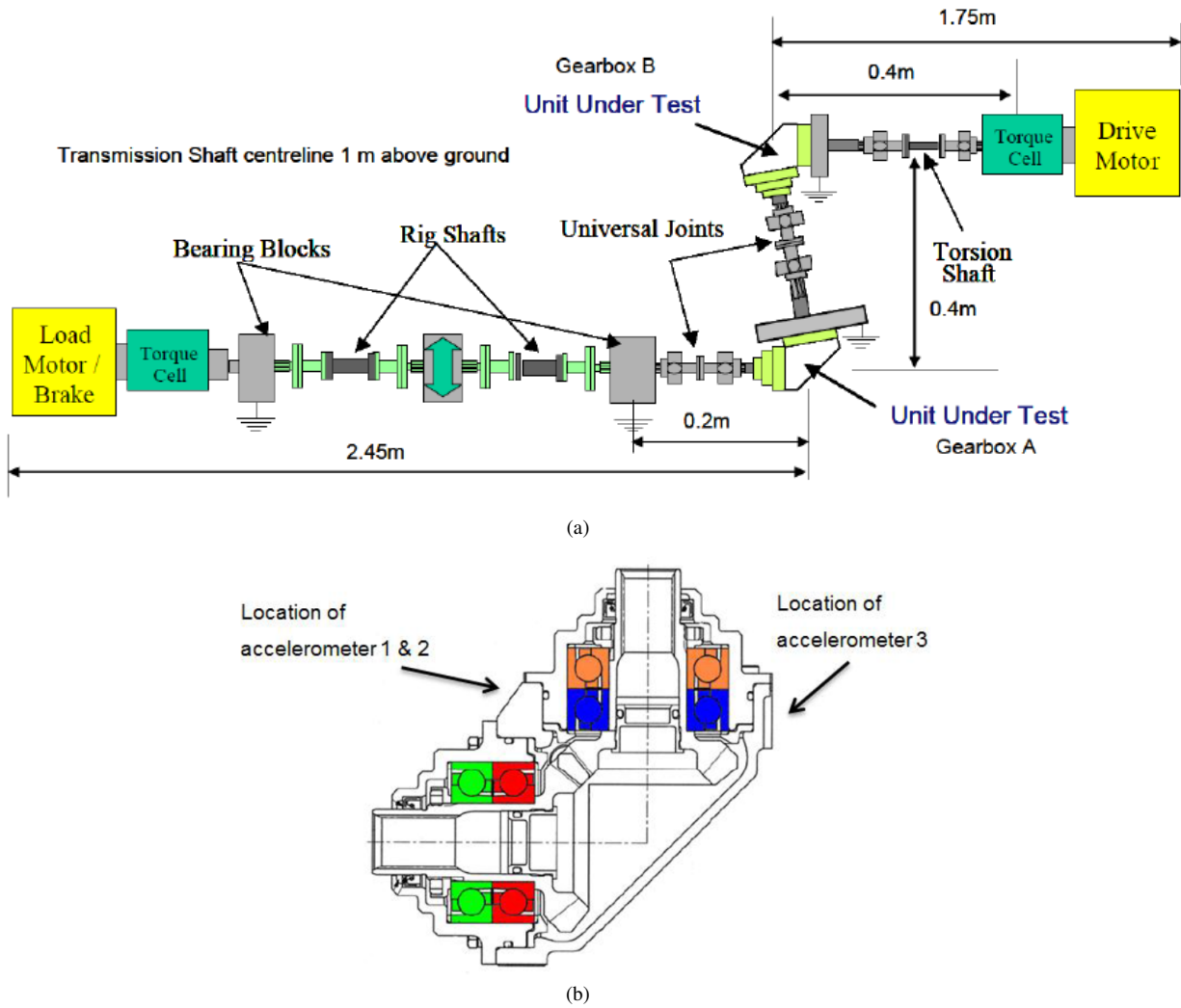


Figure 4. (a) The transmission gearbox test rig of a civil aircraft, (b) The gearbox layout and sensors location.

damage frequency (BDF) and fundamental train frequency (FTF), are listed in Table 1. All vibration data are acquired using accelerometers fixed on the outer case of the gearbox. The sampling frequency is of 5 kHz.

Table 1. Theoretical bearing fault frequencies for dataset#1.

Rotation speed	Fault frequencies [Hz]	
	60 rpm	710 rpm
BPFI	7.03	83.2
BPFO	4.96	58.8
BDF	4.37	51.2
FTF	0.41	4.9

### 3.1.2. Test rig#2

Dataset#2 has the particularity of being measured on a multiple-shaft gearbox. These data were used for the PHM09 data competition on gearbox fault diagnosis. The gearbox test setup used for generating these data is depicted in Figure 5. On this gearbox setup, two different gear geometries can be used including spur and helical gears. The dataset analyzed in this paper is collected for which the gearbox is assembled with spur gears. The gearbox configuration is as follows:

- Input shaft: input pinion of 32 teeth,
- Idler shaft: 1st idler gear of 96 teeth,
- Idler shaft: 2nd (output) idler gear of 48 teeth,
- Output shaft: output pinion of 80 teeth.

Vibration data are acquired by means of two Endevco 10 mV/g accelerometers (Sensor resonance frequency > 45 kHz). One of the two accelerometers is mounted on the input shaft side and the other one is mounted on the output shaft side. The external load is applied thanks to a magnetic brake. Data are sampled synchronously from the two accelerometers. The sampling frequency is of  $\frac{200}{3}$  kHz. A tachometer generating 10 pulses per revolution is attached on a properly selected location. The vibration signal analyzed here was collected at 50 Hz shaft speed, under high loading. The characteristic fault frequencies of the bearing of interest are given in Table 2 for two speeds.

Table 2. Theoretical bearing fault frequencies for dataset#1.

Rotation speed	Fault frequencies [Hz]	
	60 rpm	3000 rpm
BPFI	4.947	247.4
BPFO	3.052	152.6
BDF	3.984	199.2
FTF	0.382	22.89

## 3.2. Results and discussion

Data from the two test rigs have been processed to remove discrete components using the different methods presented

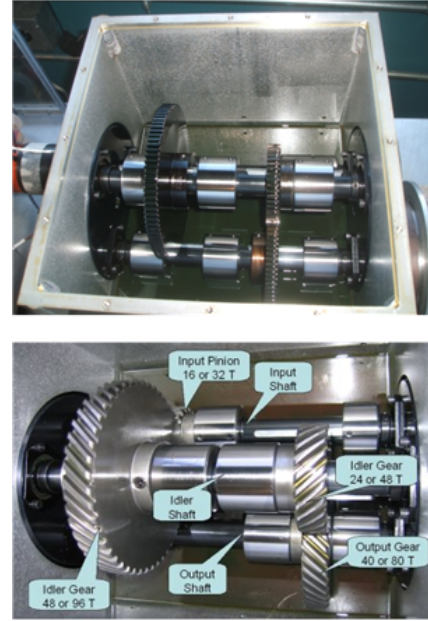


Figure 5. Gearbox diagnosis setup used in the PHM09 data competition.

above. The residual signals containing non deterministic components are further processed using the envelope analysis proposed in R. B. Randall (2011). Note that the demodulation frequency band used in the envelope analysis is determined by means of spectral kurtosis analysis using the fast kurtogram algorithm (Antoni, 2007).

### 3.2.1. Fault indicator

To assess the performance of bearing fault detection, a fault indicator is defined as the amplitude of peak at the fault frequency normalized with respect to the DC value in the envelope spectrum. In dataset#1, the concerned fault is a bearing outer race fault while the fault present in dataset#2 is located on the inner race.

### 3.2.2. Analysis of dataset#1

The SANC is performed with different values of delay and filter length. The step size is kept equal to 0.01. The delay  $L$  is chosen among the following values: 100, 200, 500, 1000, 1500, 2000, 5000 and 10000, while the filter length  $M = 12$ . The results show the best performance with  $L = 100$  as shown in Figure 6 (i.e. highest fault indicator value). Then this best delay value is used with various filter lengths to calculate the corresponding fault indicator values as shown in Figure 7.

The cepstrum editing method is also applied to dataset#1 with different normalized liftering widths chosen among the following values: 0.02, 0.04, 0.08, 0.16 and 0.32. It is important to notice here that the *normalized liftering width* is de-

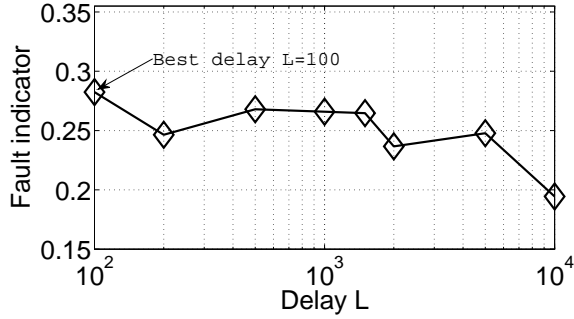


Figure 6. Effect of SANC delay on bearing fault indicator.

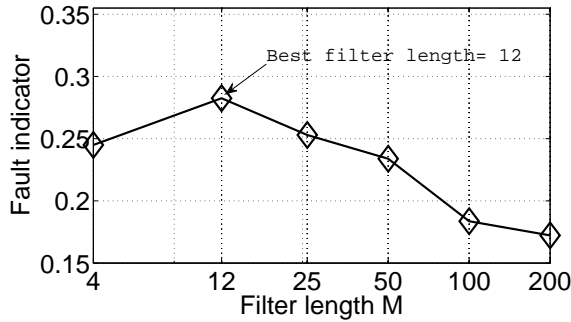


Figure 7. Effect of SANC filter length on bearing fault indicator.

defined as the ratio of the lifter width with respect to the period of discrete component of interest. The fault indicator values corresponding to the selected liftering widths are shown in Figure 8.

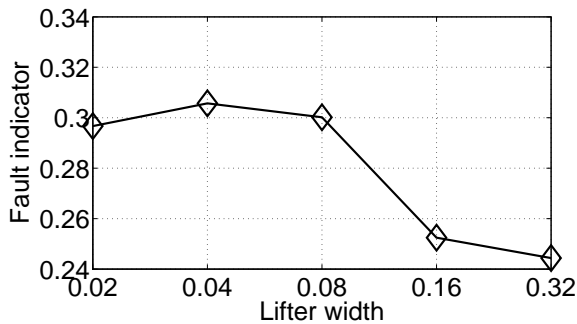


Figure 8. Effect of cepstrum editing lifter width on bearing fault indicator.

The results obtained with TSA using different number or shaft revolutions per segment are shown in Figure 9. By analyzing the best fault indicator values resulting from the above different DCR methods, it comes that the cepstrum editing method gives the best fault indicator. Figure 10 shows the envelope spectra of residuals signals obtained for the 3 DCR methods. One can notice the low background noise achieved with the cepstrum editing method. This can be also concluded by observing the kurtosis values of the corresponding residual sig-

nals listed in Table 3. As shown in Figure 11, the cepstrum editing method leads to the most impulsive residual signal.

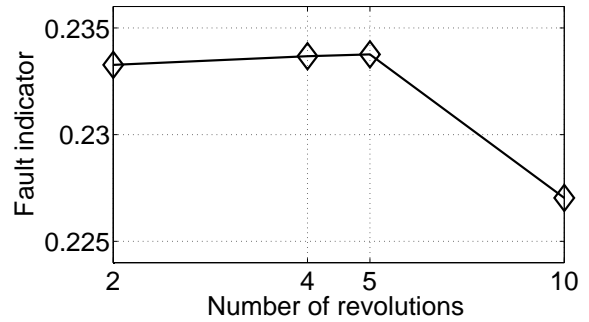


Figure 9. Effect of TSA number of revolutions on bearing fault indicator.

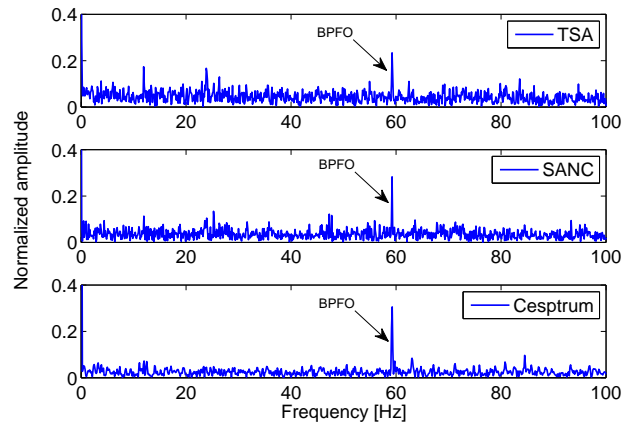


Figure 10. Comparison of envelope spectrum for dataset#1.

Table 3. Kurtosis of the residual signals of dataset#1.

	Kurtosis
TSA residual	4.0158
SANC residual	4.3990
Cepstrum residual	5.0627

### 3.2.3. Analysis of dataset#2

Similar to the analysis on dataset#1, the SANC is performed with different values of delay and filter length. The step size is kept equal to 0.01. The delay  $L$  is first chosen among the following values: 100, 200, 500, 1000, 1500, 2000, 5000 and 10000 while the filter length  $M = 12$ . The results show the best performance with  $L = 2000$  as shown in Figure 12. Then this best delay value is used with varying filter length to calculate the fault indicator as shown in Figure 13.

The cepstrum editing method is applied to dataset#2 with different liftering widths chosen among the following values:

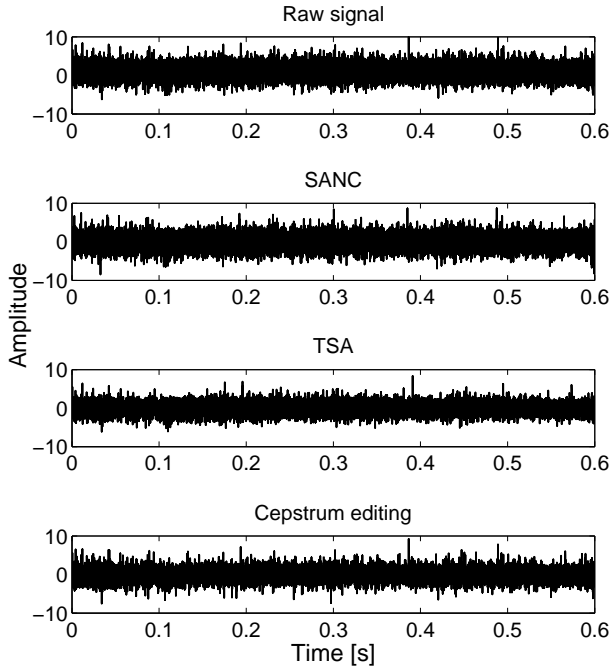


Figure 11. Normalized residual signals for dataset#1 obtained after applying 3 DCR methods.

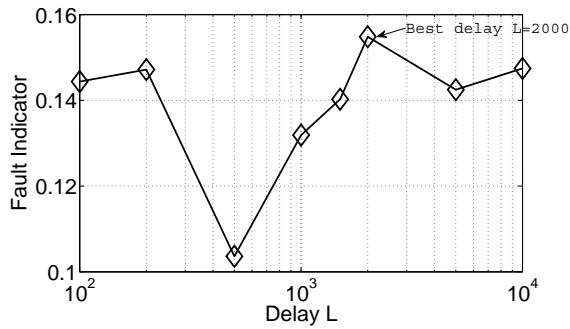


Figure 12. Effect of SANC delay on bearing fault indicator for dataset#2.

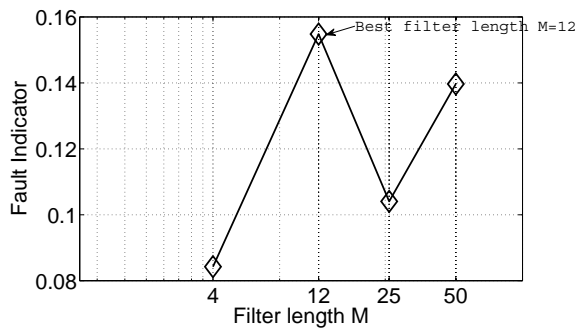


Figure 13. Effect of SANC filter length on bearing fault indicator for dataset#2.

0.02, 0.04, 0.08, 0.16 and 0.32. Subsequently, the fault indicator values for the corresponding liftering widths are calculated as shown in Figure 14.

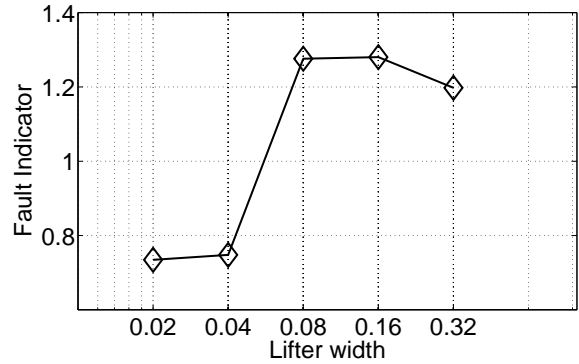


Figure 14. Effect of cepstrum editing liftering width on bearing fault indicator.

The result obtained with TSA using different number or shaft revolution per segment is shown in Figure 15. In line with the results obtained from dataset#1, the cepstrum editing method also provides the best performance for dataset#2. Figure 16 shows the envelope spectra of residuals signals obtained for the 3 DCR methods. It is seen in the figure that the cepstrum editing method highlights the fault frequency better than the other methods. The kurtosis values of the corresponding residual signal are given in Table 4. This indicates that the cepstrum editing leads to the most impulsive signal as it can also be seen in Figure 17.

Table 4. Kurtosis of the residual signals of dataset#2.

	Kurtosis
TSA residual	3.9653
SANC residual	4.0478
Cepstrum residual	6.7035

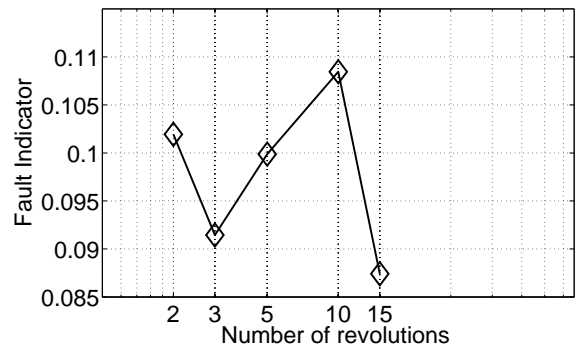


Figure 15. Effect of TSA number of revolutions on bearing fault indicator.

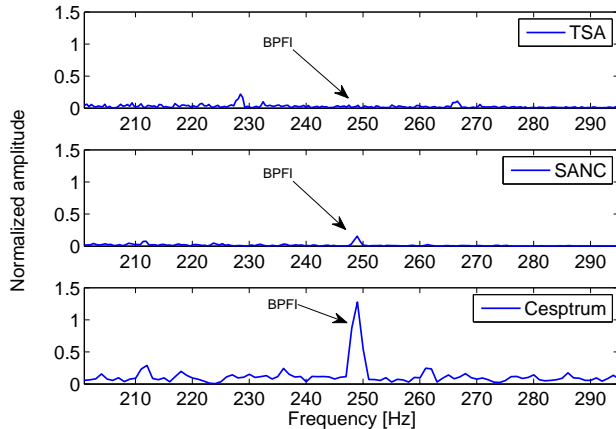


Figure 16. Comparison of envelope spectrum for dataset#2.

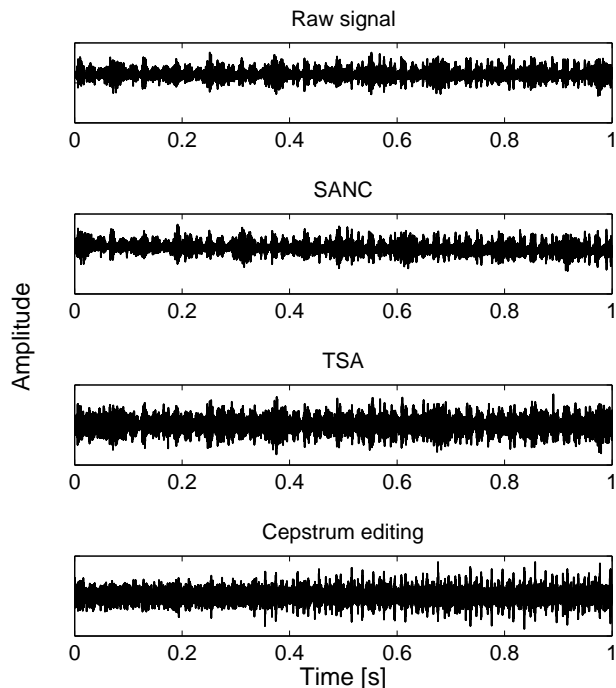


Figure 17. Normalized residual signals for dataset#2 obtained after applying 3 DCR methods.

#### 4. CONCLUSION

The performance of three different discrete component removal (DCR) methods, namely (i) time synchronous averaging (TSA), (ii) self adaptive noise cancellation (SANC) and (iii) cepstrum editing, has been quantitatively compared in this paper. For the comparison purposes, two metrics, i.e. the peak values at the fault frequencies of the envelope spectrum and the kurtosis of the time domain signal, were considered. These metrics have been extracted from the vibration signals measured on industrial and laboratory gearboxes by apply-

ing the three DCR methods with different parameter settings. The optimal parameter setting of each DCR method was deduced by visual inspection on the values of the two metrics. The higher the metric value is, the better the performance of a DCR method will be. The experimental results show that the values of the two metrics based on the cepstrum editing method are higher than those of the other two DCR methods. This suggests that the cepstrum editing method outperforms the other considered methods.

#### REFERENCES

- Antoni, J. (2007). Fast computation of the kurtogram for the detection of transient faults. *Mechanical Systems and Signal Processing*, 21(1), 108 - 124.
- Antoni, J., & Randall, R. (2004). Unsupervised noise cancellation for vibration signals: part i evaluation of adaptive algorithms. *Mechanical Systems and Signal Processing*, 18(1), 89–101.
- Bogert, B. P., Healy, M. J., & Tukey, J. W. (1963). The quefrency analysis of time series for echoes: Cepstrum, pseudo-autocovariance, cross-cepstrum and saphe cracking. In *Proceedings of the symposium on time series analysis* (pp. 209–243).
- Bonnardot, F., El Badaoui, M., Randall, R., Daniere, J., & Guillet, F. (2005). Use of the acceleration signal of a gearbox in order to perform angular resampling (with limited speed fluctuation). *Mechanical Systems and Signal Processing*, 19(4), 766–785.
- Gao, Y., & Randall, R. (1996). Determination of frequency response functions from response measurements. ii. regeneration of frequency response from poles and zeros. *Mechanical systems and signal processing*, 10(3), 319–340.
- Randall, R., & Sawalhi, N. (2011). A new method for separating discrete components from a signal. *Sound and Vibration*, 45(5), 6.
- Randall, R., Sawalhi, N., & Coats, M. (2011). A comparison of methods for separation of deterministic and random signals. *International Journal of Condition Monitoring*, 1(1), 11–19.
- Randall, R. B. (2011). *Vibration-based condition monitoring: industrial, aerospace and automotive applications*. John Wiley & Sons.
- Sawalhi, N., & Randall, R. (2011). Signal pre-whitening using cepstrum editing (liftering) to enhance fault detection in rolling element bearings. In *Proceedings of the 24 international congress on condition monitoring and diagnostic engineering management (comadem2011)*, may (pp. 330–336).
- Widrow, B., Hoff, M. E., et al. (1960). Adaptive switching circuits.